ON THE OPTIMIZATION OF THE NON-LINEAR PERFORMANCE OF 4th-GENERATION LIGHT SOURCES *

B. Kuske†, B. Alberdi-Esuain, Helmholtz-Zentrum Berlin, Berlin, Germany

Abstract

The successful non-linear performance of 4th-generation light sources can be supported through a proper design of the linear lattice. However, important quantities like the injection efficiency and the beam lifetime depend on the optimization of non-linear magnetic fields in the lattice like sextupoles and octupoles, and therefore on numerical optimization. The underlying quantities to be maximized are the limits of stable particle motion in the injection plane, the horizontal dynamic aperture, and the Touschek lifetime, i.e. the momentum acceptance of the ring. Commonly, multi-objective genetic algorithms are used for the direct optimization of the dynamic aperture and momentum acceptance. Alternatively, the resonance driving terms can be minimized. Both approaches need to take the uncertainties introduced by manufacturing tolerances and misalignment in the real machine into account. Using the parameters of the BESSY III storage ring project at HZB, Berlin, this paper compares both approaches and tries to develop an efficient optimization strategy for the upcoming technical design phase of BESSY III.

INTRODUCTION

HZB is preparing to build a 2.5 GeV storage ring as a replacement for BESSY II in the mid 2030s. BESSY III will utilize a multi-bend achromat (MBA) lattice (Fig. 1) to reach an emittance of 100 pm rad to satisfy the users demand for diffraction limited light at 1 keV. Much care has been taken to prepare a promising non-linear performance already in the development of the linear lattice [1]. Phase advances between sextupoles have been set to cancel the resonance driving terms (RDTs) and realise a higher-order achromat (HOA) lattice [2, 3]. The magnetic arrangement was chosen such, that the sextupole strength necessary to compensate for the natural chromaticity is minimal. Small emittance is reached by an optimal use of reverse bends, rather than by strong focusing. Nevertheless, the non-linear performance depends not only on the suppression of resonances, but also on confining the detuning, i.e. the tune's motion for large amplitudes and momentum offsets. This can be achieved by splitting up the initial two chromatic sextupole families into individual circuits and numerically finding an optimum between the robust performance of an HOA lattice with its reduced dependency on tolerances and sufficient momentum acceptance (MA) and dynamic aperture (DA). The MA is of paramount importance for BESSY III, to reach a long Touschek lifetime, important for operational flexibility across various user modes. The DA has to provide a sufficiently large area for injection. This paper investigates how the simultaneous reduction of the RDTs and the detuning terms can be used to define a promising sextupole scheme.

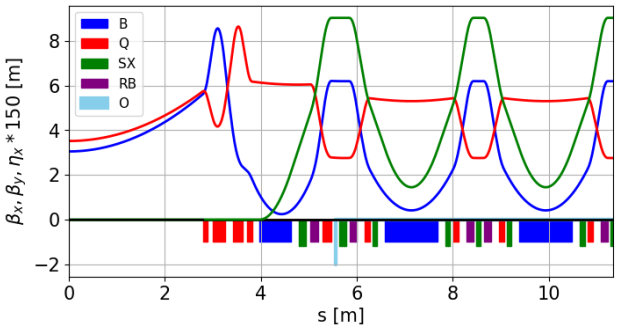

Figure 1: Half of a super period of the BESSY III lattice: $\beta_{x,y}$: blue, red, η_x: green. There is one chromatic octupole (light blue) and no harmonic multipole so far.

The results are compared to those found by multi-objective genetic optimization (MOGA).

SHORT INTRODUCTION TO DRIVING TERMS

The idea to place sextupoles with a certain phase advance between them to cancel non-linear effects originates in the 1970's, one early paper being [4], where transport matrices were used. A general treatment based on Hamiltonian formalism was derived in [5]. Based on [6], a closed form for RDTs applicable to storage rings was developed in [3], and is widely used today.

Following [7], let Eq. (1) be the Hamiltonian of the particle motion in an accelerator,

$$H(x,p_x,y,p_y;s) = \frac{p_x^2+p_y^2}{2(1+\delta)} - \frac{x\,\delta}{\rho} - \frac{x^2}{2\rho^2} + \mathrm{Re}\sum_{n=1}^{M}\frac{k_n+ij_n}{(n+1)!}(x+iy)^{n+1}, \quad (1)$$

with x, y the transverse particle positions, p_x, p_y canonical momentum conjugate to x and y, δ the relative momentum deviation, ρ the bending radius of the reference trajectory, and k_n and j_n the normal and skew multipole strengths of order n. The first three terms describe the solvable linear part of the system and the real part of the complex sum describes the perturbative part due to the non-linear elements in the ring. It is common to change to normalised coordinates and then to a resonance basis: $z^{\pm} = \sqrt{2J_z}\,e^{\pm i\phi_z} = z \mp ip_z$, with $z = x, y$, and ϕ_z the phase advance. Using this basis, and summing up over all elements in the ring, the n^{th} order

* Work supported by German Bundesministerium für Forschung, Technologie und Raumfahrt, Land Berlin, and grants of Helmholtz Association
† bettina.kuske@helmholtz-berlin.de

Hamiltonian can be expanded as

$$h^{(n)} = \sum_{\substack{j,k,l,m,p>0 \\ j+k+l+m+p-1=n}} h_{jklmp}\,(x^+)^j(x^-)^k(y^+)^l(y^-)^m\delta^p \quad (2)$$

The h_{jklmp} are called resonance driving terms, as they can lead to resonant behaviour due to their amplitude and phase dependant contribution to H. Not every term drives resonances, though: the second order terms $h^{(2)}_{11001}$ and $h^{(2)}_{00111}$ drive the linear chromaticity, third order terms $h^{(3)}_{22000}$, $h^{(3)}_{00220}$ and $h^{(3)}_{11110}$ drive the tune shift with amplitude. Therefore, this paper uses "driving terms" (DTs) to cover all Hamiltonian orders. All DTs, can be expressed as analytic functions of the magnet data and the linear lattice functions, including $\delta\beta/\delta p$, $\delta\eta/\delta p$, and $\delta\eta/\delta s$. The (rather complicated) formulas have been derived among others in [3, 8, 9]. This paper uses the formulas given in [3, 8].

If $p = 0$, i.e. the on-momentum case, the DTs are called geometric, if $p \neq 0$ chromatic. Not all DT have a dependence on the phases. Phase dependent DTs can be reduced by explicitly choosing the phase advance between the sextupole kicks. For perfect matching they would be zero. The need to cancel the dispersion function in the straight section of a MBA lattice inevitability prohibits this, but the respective DTs remain small.

In this work, only the geometric and chromatic DTs of second order ($j + k + l + m = 3$) and the third order terms causing tune shift with amplitude and momentum are evaluated and minimized. To this end, the freedom arising from splitting up the two chromatic sextupole families in the arc into individual, but symmetric circuits is exploited, rather than adding further non-linear elements, with the exception of two octupoles, placed symmetrically close to the outer dipoles.

THE MINIMIZATION PROCEDURE

The goal of minimizing the DTs is to find the optimum between the robustness of the HOA lattice against errors and the confinement of the tune's movement with particle amplitudes and energy deviation. The BESSY III sextupoles can be powered in 8 individual families, while keeping the symmetry in each arc. This flexibility is used to minimize the DTs. The lattice performance is assessed by the size of the DA and MA.

The minimization algorithm has to utilize constraints, to avoid dependence on the choice of the chromaticity compensating sextupoles. The COBYLA algorithm [10, 11] allows for constraints suitable for adjusting the chromaticity $\xi_{x,y}$ to the desired value. COBYLA showed the fastest and most reliable performance of different minimization routines tested. Global minimization algorithms were not considered, due to their slow convergence.

All linear lattice and magnet data are collected once at the beginning and stored in a data frame. The minimization procedure works exclusively on that data frame, without further lattice evaluations. DTs might vary by orders of magnitude in size. A weight function taken from [12], Eq. 71, leverages their magnitude before minimization.

The minimization concentrates on four 'classes' of DTs. Geometric and chromatic DTs (2nd order Hamiltonian) and the amplitude (TSWA) and momentum (TSWM) driven tune shift terms (3rd order). Higher-order DTs partly depend on the lower orders, and will be automatically reduced. The DTs of each class represent different physical phenomena. In the minimization, the RMS-value of the terms in each class is used. This is justified for a general minimization. When specific resonances or detuning needs to be suppressed, individual DTs have to be considered. To this end, a further weight function, a simple factor for each individual DT is introduced that allows to emphasis single DTs or complete classes. The optimizer's goal function is the sum of the RMS values of the four classes.

Each minimization starts with the HOA-case, i.e., 16-fold symmetry, no errors, two families of sextupoles (SD, SF) of equal integrated strength and $\xi_{x,y} = 1$.

In each iteration, the DTs are derived for the new set of sextupole values and the goal function is calculated. After convergence, the DA and the MA are calculated for the optimized set of sextupole values using 6D-tracking (1024 turns) in pyAT [13]. As the lattice does not incorporate errors, a detuning limit is used to mimic 'particle loss'. A limit of $\sqrt{Q_x^2 + Q_y^2} < 0.04$ on the tune shift is applied (determined in preliminary studies). The DA is represented by its area. The minimal stable horizontal amplitude is recorded, important for injection from the inside of the ring. The MA is the local MA in the straight section.

MINIMIZATION RESULTS

The HOA-case

The BESSY III lattice realisation with only two sextupole families with equal integrated strength is called the "HOA-case". The DTs of interest for this case are listed in Table 1. The second order terms are not exactly zero, but small, as explained above. The TSWA terms are strongly dominant.

Table 1: Driving Terms of the HOA-case

class	DT	value
geometric	h_{21000}, h_{30000}	3.71, 2.41
	h_{10110}, h_{10020}	1.04, 4.75
	h_{10200}	5.14
chromatic	h_{20001}, h_{00201}	1.81, 0.94
	h_{10002}	0.0
TSWA	h_{22000}, h_{00220}	-187643, -62524
	h_{11110}	-54343
TSWM	h_{11002}, h_{00112}	36.58, 12.16

Table 2 lists the RMS-values for each DT class without weights and when the weights to leverage magnitudes are applied. Despite the weighting, the TSWA still is dominant and weights are used during minimization to boost the TSWM terms.

Table 2: RMS and Weighted RMS Values for Each DT Class for the HOA-case

class	RMS	weighted RMS
geometric	3.73	0.086
chromatic	1.18	0.257
TSWA	118424	14.46
TSWM	27.26	0.324

For a tune shift limit of 0.04, the HOA-case has a MA of 3.4 %, an area of the DA of 3.2 mm^2 at $\beta_{x,y}$-function of 3.2 m, 3.6 m, respectively, and a minimal stable x-amplitude of 1.2 mm, all not sufficient for the BESSY III goals.

Deviations from the HOA

To illustrate the effect of the phase matching, the DA of the HOA-case is calculated by tracking for 10 different error sets, based on the values in Table 3. The resulting orbit distortion is corrected, but not the residual β-beat. The DA of the HOA-case is very insensitive towards errors, see Fig. 2 (left). Figure 2 (right) shows the DA, when a 20 percent deviation of the sextupoles strengths from the HOA-case is allowed during minimization of the DTs. Clearly, errors have a much larger effect. The larger the deviation is from the HOA-case, the smaller the detuning terms, the larger is the DA, but also the sensitivity towards errors increases. The black lines in Fig. 2 mark the mean DA.

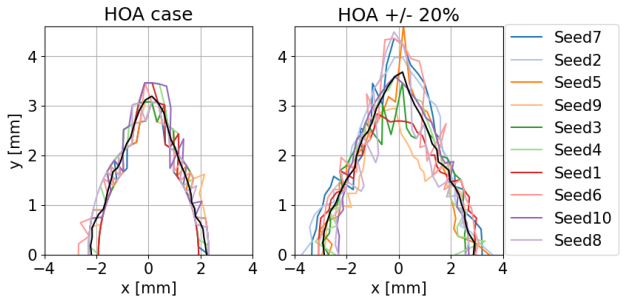

Figure 2: Left: the DA of the HOA-case for 10 sets of errors. Right: DA when allowing for a 20 % deviation of the sextupole strength in the DTs minimization.

Table 3: Standard RMS Tolerances

transverse misalignment (all magnets)	30 µm
roll (all magnets)	180 µrad
pitch and yaw - dipoles	60 µrad
pitch and yaw - other magnets	400 µrad
calibration	1e-4

Increasing the DA

The DT minimization (DTM) is performed for a stepwise increasing limit, 10 % to 40 %, on the deviation of the 8 sextupole family strengths from the HOA-case values. Nine weights (1, 50, 100, ..., 400, 450) are applied to leverage between TSWA and TSWM. In addition, six discrete strengths of the symmetrically placed octupole, Fig. 1, are used, from 0 m^{-3} to 500 m^{-3}. Octupoles only contribute to the 3rd order Hamiltonian terms (and larger), by adding

$$h_{\mathrm{iijj0}}\,(oct) \propto \oint k_3 \beta_x^i \beta_y^j ds \qquad i,j = (2,0),(0,2),(1,1)$$

to the TSWA, where k_3 is the integrated octupole strength.

The contribution to the TSWM terms is

$$h_{\mathrm{iijj2}}\,(oct) \propto \oint k_3 \beta_x^i \beta_y^j \eta_x^2 ds \qquad i,j = (1,0),(0,1).$$

Figure 3 shows the area of the DA over the MA for sextupole settings obtained by DTM for six octupole strengths (colors), and 9 weights (symbol size), each, and limits on the sextupole strength deviation from the HOA-case, with ± 10 % (dots), ± 20 % (triangles), ± 30 % (squares), and ± 40 % (crosses). The RF acceptance lies at ≈ 6.25 %. While the 10 % case can increase the MA to the RF limit, it takes at least 20 % deviation to also increase the DA.

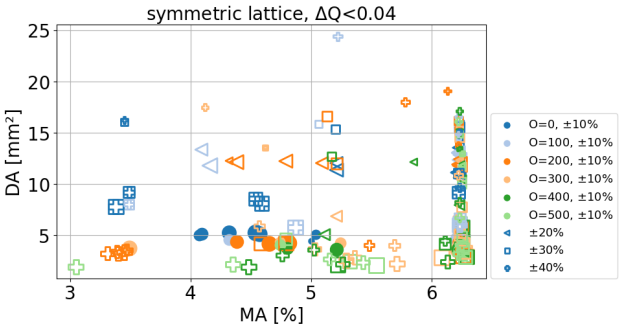

Figure 3: DA over MA for 4 limits on the deviation from the HOA-case sextupole strengths: 10 % (dot), 20 % (triangle), 30 % (square), and 40 % (cross). Colours mark octupole strengths [m^{-3}] and symbol sizes mark different weights.

DA and MA in Fig. 3 are calculated using the tune shift limit in the tracking. It has to be verified, how much reduction occurs when the related multipole strengths are used in lattices where magnet tolerances are applied.

The 10 best cases of Fig. 3 were (somewhat arbitrarily) defined by MA > 6.0 % and DA > 15.2 mm^2, and have 20 %, 30 % or 40 % deviation from the HOA-case. They have each been applied in 10 misaligned lattices (100 cases), with corrected orbit, but no β-beat correction. The stability criteria in tracking with errors is particle loss. Table 4 lists the mean values of the best 10 results (bare lattice, tune shift limit) and the statistics of 100 calculations including tolerances: mean, standard deviation, and the reduction with respect to the bare lattice.

Table 4: 16-fold Symmetry, Tune Shift Limit=0.04

		bare lattice	including tolerances		
		DTM	mean	std	reduction
MA	%	6.22	5.21	0.31	-16%
DA	mm^2	16.28	11.85	2.93	-27%
x_{min}	mm	-2.76	-2.62	0.49	-5%

There are further losses due to the excited resonances, but the MA above 5 % could be confirmed, and the losses

of 27 % in the DA mainly occur in the vertical plane, as the minimal stable horizontal amplitude varies only by 5 %. Nevertheless, a larger acceptance is needed for injection.

Including the Injection Straight

BESSY III will utilize a modified injection straight [14]. A non-linear kicker (NLK) will be installed between the two parts of the devided 2nd quadrupole in the straight section, and the 1st quadrupole is shifted towards the two septa, see Fig. 4. The injected beam propagates to the NLK, where it is kicked into the stored beam's acceptance. At the NLK $\beta_x = 11.9$ m.

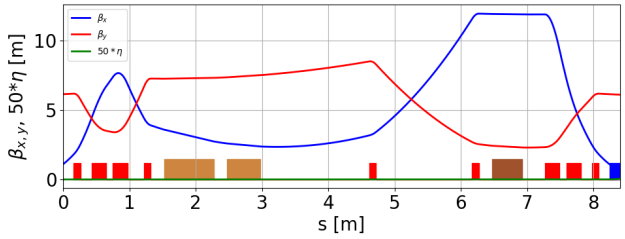

Figure 4: The modified injection straight with the thick and thin septa (light brown) and the NLK (brown).

The changes in the injection straight break the symmetry of the 16-fold lattice. To reduce effects on the non-linear performance, the phase advance across the injection straight is kept constant. Nevertheless, the super periodicity is one and the chromatic DTs differ from the periodic lattice as they include K_1, $\beta_{x,y}$ and $\frac{d\beta_{x,y}}{ds}$. Therefore, the minimizer will find different solutions.

As above, Fig. 5 shows the results of the rough scan over octupole strengths and weights, for 10 % to 40 % deviation from the HOA-case. The 10 best results were (again somewhat arbitrarily) defined by choosing the largest DAs with a MA > 5.4 %. The integrated octupole kicks of these cases concentrate around 200 m^{-3}, see Fig. 6. The deviation from the HOA-case is 30 % for 9 cases and 40 % for one case.

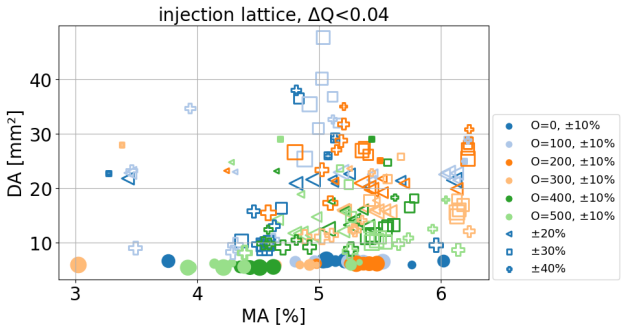

Figure 5: DA and MA at the NLK for 10 % (dots), 20 % (triangle), 30 % (square), and 40 % (cross) allowed deviation from the HOA. Colours mark different octupole strengths and symbol sizes mark different weights

Again, ten different error realisations have been used to confirm the results for the most promising multipole configurations. Table 5 shows the mean of the 10 best results,

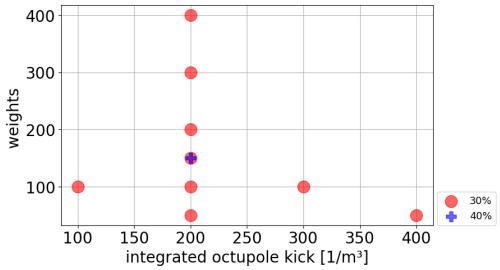

Figure 6: Scan parameters of the 10 best results.

(bare lattice, tune shift limit) and the mean values and standard deviations when 10 error sets each are applied (100 cases), and the loss compared to the bare lattice; the orbit, the β-beat and the coupling were corrected. The MA is stable above 5 %, and the DA even increases, indicating that the tune limit of 0.04 is too tight for the TSWA. For the averaged multipole strengths, of these 10 cases, simulated commissioning predicts an injection efficiency 97 % [15].

Table 5: Injection Lattice, Tune Shift Limit=0.04

		bare lattice	including tolerances		
	unit	DTM	mean	std	reduction
MA	%	5.93	5.29	0.17	-11%
DA	mm^2	27.53	39.48	3.00	+43%
x_{min}	mm	-8.88	-8.60	0.66	-5%

MOGA OPTIMIZATION OF DA AND MA

Multi-objective genetic algorithms, MOGA, are a common choice to optimize many parameters for multiple goal functions. They have the advantage that theoretically very complex physical models can be simulated. Their drawback is the large CPU and time consumption.

In this study, MOGA runs directly optimize the DA and MA. They use the *NSGA-II* algorithm of the *Python pymoo* package [16]. The physics is covered by *pyAT* and *pySC* [17]. The runs start from the linear lattice, with eight distinct, but symmetric sextupole families, and a single octupole. Before optimization, the errors presented in Table 3 are applied to the lattice, the orbit is corrected. Magnet values are confined to their technical limits and a constraint function pins the chromaticity to $\xi_{x,y} = 1$. Full 6D tracking is performed for 1024 turns, and the MA and DA at the NLK ($\beta_x = 11.9$ m) are defined by particle loss. Physical apertures of ± 9 mm are applied around the ring to avoid non-relevant results. With a population of 300 points, each generation of the genetic algorithm produces 100 off-springs, and the optimization runs for 200 generations. For each generation, the population and the off-springs are evaluated according to their result in the objective space, and the 100 points with the worst results are discarded. A run takes around 20 hours on 100 CPUs of an HPC.

Figure 7 shows the resulting Pareto fronts for 10 different error sets. Most solutions show MAs > 4.5 %, and DAs between 30 mm^2 and 50 mm^2. As in the DTM the most promising result within each Pareto front is defined by the

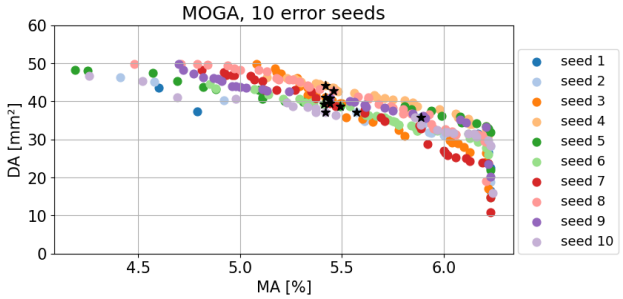

Figure 7: Pareto front for 10 different error sets. Best results are marked by a star.

maximum DA with a MA ≥ 5.4 % and marked by a black star. The octupole strength of the best cases varies between 82 m^{-3} and 330 m^{-3}.

In the MOGA runs, the MA and DA are optimized for a specific error set, which will unlikely be that of the real machine. Therefore, also each MOGA result is evaluated across multiple error realisations to assess consistency. Table 6 lists the mean of the best results of the 10 Pareto fronts, and the statistical values when the related magnet strengths are applied to 10 error realisations each (100 cases).

Table 6: MOGA Results Best DA for MA > 6.0 %

		MOGA	different tolerances		
	unit		mean	std	reduction
MA	%	5.50	5.44	0.33	-1%
DA	mm^2	39.65	27.71	5.98	-43%
x_{min}	mm	-	-6.48	1.04	-

COMPARISON

The MOGA-MA is slightly larger than the DTM-MA, but the DA and the stable range for injection is significantly larger in the DTM. Stable minimal amplitudes of −8.6 mm on average are sufficient for injection with a maximal NLK-amplitude at −7 mm. A MA larger 5 % provides sufficient lifetime. To further compare both strategies, the multipole strengths of the 10 best cases and the related DTs are looked at. Figure 8 displays the absolute integrated sextupole strengths of the best MOGA results (light-blue) and their mean (blue), the best DTM results, (light-green) and their mean (green), and the HOA values (black). Both approaches allocate a significant portion of the sextupole fields in the outer two sextupoles S1 (defocusing) and S2 (focusing), compared to the HOA configuration. The DTM results are more confined than the MOGA results, with mean individual standard deviations of 3.9 %/7.8 %, respectively. The mean S1 and octupole strengths are stronger in the MOGA results, with values of −34.6 m^{-2}/−27.5 m^{-2} and 243 m^{-3}/220 m^{-3}, respectively.

Table 7 displays the weighted DTs of the mean multipole strengths of both approaches. The small TSWA terms of MOGA indicate, that the DA reduction is due to higher order DTs.

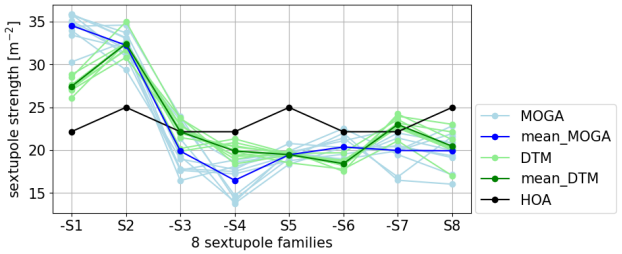

Figure 8: The integrated sextupole strengths of the best results of MOGA (light-blue), and DTM (light-green), the mean values (blue, green), and the HOA values (black).

Table 7: DTs for the mean resulting multipole strengths of MOGA and DTM. All values are for the injection lattice.

DT class	MOGA	DTM	HOA
geometric	0.41	0.35	0.10
chromatic	0.11	0.17	0.23
TSWA	3.151	5.96	16.36
TSWM	0.27	0.26	0.18

CONCLUSION

The paper presents an efficient method of DTM and compares the results to MOGA calculations for the BESSY III lattice. The DTM only considers 3rd order resonance DTs, TSWA- and TSWM terms, i.e. 4 classes of DTs. The results show a clear advantage for the DTM in DA and stable injection range. In both cases, the results depend on the choice of the 'best cases' in the result space.

The advantage of DTM in practical work is the runtime of <1/10 of the MOGA runtime, ≈1 h to 2 h, depending on the number of iterations necessary during minimization and the size of the lattice. The MOGA runs take around 20 h. Considering the necessity to adust the non-linear configuration of the lattice repeatedly for different tunes, chromaticities, lattice modifications and the like during the development of the project, DTM will be the primary tool in the BESSY III project development.

REFERENCES

[1] B. Kuske and P. Goslawski, "Construction of multi-bend achromat lattices based on their substructures", *Phys. Rev. Accel. Beams*, to be published.

[2] J. Bengtsson, "Non-linear transverse dynamics for storage rings with applications to the low-energy antiproton ring (LEAR) at CERN", Ph.D. thesis, Lund U., Geneva, Switzerland, 1998. doi:10.5170/CERN-1988-005

[3] J. Bengtsson, "The sextupole scheme for the SLS", PSI, Villingen, Switzerland, Rep. SLS-Note 9/97, Mar. 1997.

[4] K. L. Brown, "A Second Order Magnetic Optical Achromat", *IEEE Trans. Nucl. Sci.*, vol. 26, pp. 3490–3492, 1979. doi:10.1109/TNS.1979.4330076

[5] G. Guignard, "A General Treatment of Resonances in Accelerators", CERN, Geneva, Switzerland, Rep. CERN-78-11, CERN-YELLOW-78-11, Nov. 1978. doi:10.5170/CERN-1978-011

[6] A. J. Dragt and J. M. Finn, "Lie Series and Invariant Functions for Analytic Symplectic Maps", *J. Math. Phys.*, vol. 17, pp. 2215–2227, 1976. doi:10.1063/1.522868

[7] I. Martin, "Nonlinear beam dynamics: lecture 2", Lecture slides, John Adams Institute (Hilary Term), Accessed via CERN Indico, 2020, https://indico.cern.ch/event/867138/contributions/3654252/attachments/1986241/3309741/Lecture_NLBD_2.pdf,

[8] M. E. Arlandoo, "Transverse resonance island buckets in advanced light sources", Ph.D. thesis, Humboldt-Universität zu Berlin, Berlin, Germany, 2024. doi:https://doi.org/10.18452/29179

[9] C.-x. Wang, "Explicit formulas for 2nd-order driving terms due to sextupoles and chromatic effects of quadrupoles", Chicago, IL, USA, Rep. ANL/APS/LS-330, Mar. 2012. doi:10.2172/1039519

[10] M. J. D. Powell, "A Direct Search Optimization Method That Models the Objective and Constraint Functions by Linear Interpolation", in *Advances in Optimization and Numerical Analysis*. the Netherlands: Springer, Dordrecht, 1994. doi:10.1007/978-94-015-8330-5_4

[11] "SciPy documentation", https://docs.scipy.org/doc/scipy/index.html, Accessed: May 08, 2025 Version: 1.15.3,

[12] A. Streun, "OPA Documentation: Inside OPA (inside1.pdf)", https://github.com/opa-code/opa4-documentation/blob/main/inside1.pdf, Accessed: 2026-02-28, 2024,

[13] S. White, L. Carver, L. Farvacque, and S. Liuzzo, "Status and recent developments of python Accelerator Toolbox", in *Proc. IPAC'23*, Venice, Italy, pp. 3185–3188, Sep. 2023. doi:10.18429/JACoW-IPAC2023-WEPL031

[14] M. Abo-Bakr, T. Atkinsen, P. Goslawski, and J. Völker, "The BESSY III Injection Scheme", presented at IPAC'26, Deauville, France, May 2026, paper THP2147, this conference.

[15] B. Alberdi-Esuain, M. Abo-Bakr, and P. Goslawski, "Simulated Commissioning and Lattice Robustness for BESSY III", presented at IPAC'26, Deauville, France, May 2026, paper THP2035, this conference.

[16] J. Blank and K. Deb, "Pymoo: multi-objective optimization in python", *IEEE Access*, vol. 8, pp. 89497–89509, 2020. doi:10.1109/ACCESS.2020.2990567

[17] T. Hellert, "Python Simulated Commissioning", https://github.com/ThorstenHellert/SC, Accessed: 2025-05-09,